APPLIED AND ENVIRONMENTAL MICROBIOLOGY, Oct. 1996, p. 3687–3696 Vol. 62, No. 10
0099-2240/96/$04.00+0

Physiology and Metabolic Fluxes of Wild-Type and Riboflavin-Producing *Bacillus subtilis*

UWE SAUER,[1] VASSILY HATZIMANIKATIS,[1] HANS-PETER HOHMANN,[2] MICHAEL MANNEBERG,[3] ADOLPHUS P. G. M. VAN LOON,[2] AND JAMES E. BAILEY[1]*

Institute of Biotechnology, Eidgenössische Technische Hochschule Zürich, CH-8093 Zürich,[1] and Section Biotechnology, Vitamin and Fine Chemical Division,[2] and Pharmaceutical Research-Gene Technologies,[3] F. Hoffmann-La Roche Ltd., CH-4002 Basel, Switzerland

Received 5 March 1996/Accepted 24 July 1996

Continuous cultivation in a glucose-limited chemostat was used to determine the growth parameters of wild-type *Bacillus subtilis* and of a recombinant, riboflavin-producing strain. Maintenance coefficients of 0.45 and 0.66 mmol of glucose g^{-1} h^{-1} were determined for the wild-type and recombinant strains, respectively. However, the maximum molar growth yield of 82 to 85 g (cell dry weight)/mol of glucose was found to be almost identical in both strains. A nonlinear relationship between the specific riboflavin production rate and the dilution rate was observed, revealing a coupling of product formation and growth under strict substrate-limited conditions. Most prominently, riboflavin formation completely ceased at specific growth rates below 0.15 h^{-1}. For molecular characterization of *B. subtilis*, the total amino acid composition of the wild type was experimentally determined and the complete building block requirements for biomass formation were derived. In particular, the murein sacculus was found to constitute approximately 9% of *B. subtilis* biomass, three- to fivefold more than in *Escherichia coli*. Estimation of intracellular metabolic fluxes by a refined mass balance approach revealed a substantial, growth rate-dependent flux through the oxidative branch of the pentose phosphate pathway. Furthermore, this flux is indicated to be increased in the strain engineered for riboflavin formation. Glucose catabolism at low growth rates with reduced biomass yields was supported mainly by the tricarboxylic acid cycle.

The genus *Bacillus* includes a variety of industrially important species that are commonly used as hosts in the fermentation industries (1, 20). In particular, their ability to secrete large quantities of protein directly into the medium has rendered them very attractive for commercial applications. The nonpathogenic bacterium *Bacillus subtilis* has become a model organism not only for the genus *Bacillus* but also for gram-positive bacteria in general. However, despite the extensive knowledge of *B. subtilis* genetics and biochemistry, surprisingly little information is available on the bioenergetic aspects of its growth and product formation (42). An in-depth understanding of bioenergetics, particularly the maintenance demand and its impact on product formation, may be necessary for the design of an optimal fermentation process (46). This is especially noticeable at lower growth rates, where the effects of maintenance metabolism are more pronounced relative to those of growth metabolism. Since many industrial bioprocesses are carried out in the fed-batch mode, which at later stages is characterized by very low growth rates, maintenance metabolism is of both scientific and industrial interest (39, 46, 47). In fermentations for penicillin production, for example, about 70% of the carbon source is utilized for maintenance (22).

Riboflavin (vitamin B_2), a commercially important additive used in the feed and food industries, was chosen as a model product to investigate the effects of product formation on energy conversion in *B. subtilis*. This water-soluble, yellow vitamin is synthesized from the purine building block GTP and ribulose-5-phosphate by plants and microorganisms via seven enzymatic reactions, but higher animals require it in their diet. Its biological function is as a precursor for the formation of the flavin nucleotides, which serve as prosthetic groups for many oxidoreductases (3, 35). Industrial production of riboflavin is achieved by complete chemical synthesis, wholly by microbial synthesis, or by a mixed process. On a commercial scale, various competitive fermentation processes have already been developed, usually involving the fungi *Eremothecium ashbyii* and *Ashbya gossypii* (14). A faster process involving the bacterium *B. subtilis* generally yields final product concentrations exceeding 15 g/liter (36).

In this study, the bioenergetics of growth and product formation in glucose-limited chemostat cultivations of wild-type and riboflavin-producing *B. subtilis* strains were studied. The overall amino acid composition was determined for the wild type, allowing conclusions on biosynthetic requirements for growth. The experimental data were further used in a detailed stoichiometric framework of metabolite (mass) balances to estimate the metabolic flux distribution, key variables for a rational strain development. Flux estimates are compared with the data available in the literature, and the problems inherent in this standard approach are discussed.

MATERIALS AND METHODS

Bacterial strains. Competent cells of *B. subtilis* 1012 (*leuA8 metB5*) (40) were transformed by congression, by following standard protocols (21), with chromosomal DNA from the riboflavin-producing strain RB50 *pur60* Ag^r-11 Dc^r-15 Ms^r-46 *spo0A ribC* (36). The resulting leucine prototrophic colonies were screened for sporulation-defective phenotypes. The modified *rib* operon pRF93 and the deregulating *ribC* mutation were transferred to one of the *spo* leu^+ colonies via PBS1 phage transduction. The phage lysate was obtained from the riboflavin-producing strain RB50 *pur60* Ag^r-11 Dc^r-15 Ms^r-46 *spo0A ribC*::[pRF69]::[pRF93] (36). pRF93 is a modified version of the *B. subtilis rib* operon, which is present at map position 135° of the RB50 genome, interrupting the nonessential *bpr* gene. Similar to the two modified *rib* operons pRF69 and pRF89 (36), pRF93 contains two strong, constitutive phage promoters, *spo1-15*, up-

* Corresponding author. Mailing address: Institut für Biotechnologie, ETH Hönggerberg, CH-8093 Zürich, Switzerland. Phone: 41/1/633 3170. Fax: 41/1/633 1051.

stream of *ribA* (ORF3) and *ribT* (ORF5). Downstream of pRF93, a tetracycline resistance gene was inserted for selection. RibC, encoded at map position 146°, is the flavin kinase of *B. subtilis*, and it also acts as a repressor of *rib* gene expression (8). The deregulating mutation in the *ribC* gene of PB50 was cotransduced with pRF93 and the tetracycline resistance marker. *B. subtilis* 1012 *metB5 spo0A* and 1012 *metB5 spo0A ribC*::[pRF93] were provided with a wild-type *metB5* gene and designated *B. subtilis* wild type and PRF93, respectively.

Growth conditions and media. Precultures and batch cultures were grown in baffled shake flasks with either Luria-Bertani complex medium or Spizizen's minimal salts medium supplemented with 20 mM glucose (21). Continuous cultivations in aerobic, glucose-limited chemostats were conducted at a working volume of 3 liters in a 6-liter bioreactor (LH-Inceltech, Toulouse, France), equipped with pH, dissolved-oxygen, temperature, optical density, and foam probes, at a temperature of 37°C. The medium contained (per liter of distilled water) glucose, 3.6 g; K_2HPO_4, 4 g; $(NH_4)SO_4$, 2 g; $MgSO_4 \cdot 7H_2O$, 0.2 g; and 10 ml of trace element solution with the following composition (per liter of distilled water): $CaCl_2 \cdot 2H_2O$, 0.55 g; $FeCl_3$, 1 g; $MnCl_2 \cdot 4H_2O$, 0.1 g; $ZnCl_2$, 0.17 g; $CuCl_2 \cdot 2H_2O$, 0.043 g; $CoCl_2 \cdot 6H_2O$, 0.06 g; and $Na_2MoO_4 \cdot 2H_2O$, 0.06 g. The medium was acidified to a pH between 2 and 3 by addition of 14 ml of H_2SO_4 (95 to 97%) and sterilized by being passed through a 0.2-μm-pore-size filter. The trace element solution (1:10 dilution) was added after the filtration to prevent the formation of precipitates. Antifoam (P2000) was present only during the initial batch cultivation but was not added to the chemostat medium to avoid any possible interference with bacterial membrane functions. The pH was controlled at 6.60 ± 0.05 during the fermentation. The fermentation volume was kept constant by a weight-controlled pump. A constant air flow of 2 liters/min was achieved by a mass flow controller, and the agitation speed was set to values between 600 and 1,500 rpm, ensuring dissolved-oxygen levels above 25%. Samples were taken only from chemostats in steady state, which were defined as at least 5 volume changes after adjusting to a new dilution rate and stable optical density as well as oxygen uptake and carbon dioxide production rate for minimally 1 volume change.

Analytical techniques. Fermentation broth samples were analyzed for cell dry weight, glucose, typical *Bacillus* fermentation by-products, extracellular protein, and riboflavin. Selected samples were also subjected to enzymatic analysis of ethanol, formate, pyruvate, and succinate as well as high-pressure liquid chromatography analysis of amino acids. Cell dry weight was determined from at least eight parallel 10-ml cell suspensions, which were harvested by centrifugation, washed with distilled water, and dried at 85°C for 24 h to a constant weight (±3% variation). Elemental biomass composition analysis was performed on lyophilized cells with an EA 1108 elemental analyzer (Carlo Erba Instruments, Milan, Italy). Glucose, ethanol, formate, pyruvate, and succinate concentrations were determined on a Synchron CX5CE automated enzyme analysis system (Beckman, Brea, Calif.) as described by Bergmeyer (5) with either kits supplied by the manufacturer or chemicals and enzymes purchased from Sigma, Buchs, Switzerland. Acetate, acetoin, and 2,3-butanediol were measured by gas chromatography (5890E; Hewlett Packard, Avondale, Pa.) on a Carbowax MD-10 column (Macherey-Nagel, Düren, Germany) with butyrate as an internal standard. A kit from Bio-Rad, Munich, Germany, was used for the determination of extracellular protein in the supernatant. For riboflavin measurements, 0.8 ml of culture broth was mixed with 0.2 ml of 1 M NaOH. A 0.4-ml volume of the resulting solution was neutralized with 1 ml of 0.1 M potassium phosphate buffer (pH 6.0), and the A_{444} was measured. Concentrations of oxygen and carbon dioxide in the off-gas were determined with either a quadrupole mass spectrometer (Fisons, Uxbridge, United Kingdom) or an emission monitor (no. 3427; Brüel & Kjær, Nærum, Denmark).

Amino acid composition analysis. Bacterial cell pellets were dried in a vacuum oven over P_2O_5 at 80°C for 24 h. Samples weighing approximately 4 to 5 mg were placed in a 4-ml long-neck glass vial with 1.7-mm-thick walls. After addition of 1 ml of 6 M HCl in 0.02% phenol, the solution was frozen in dry ice and evaporated at below 1.3 kPa for 3 min, and the vial was sealed by melting while still under vacuum. The samples were then hydrolyzed at 110°C for 24 or 72 h and subsequently dried under vacuum in a desiccator. The residues were dissolved in a diluent buffer (pH 2.2), and aliquots were withdrawn for analysis. Amino acid analysis was performed by a modification of the method of Spackman et al. (43) on a Kontron Liquimat III amino acid analyzer. The amino acids were separated on a cation exchanger (CK10F; Mitsubishi Kasei Corp.) and eluted with a step gradient from 0.16 to 0.35 M sodium citrate (pH 3.21 to 4.24). The elution was monitored by recording the A_{440} and A_{570} of the ninhydrin derivatives. Elution profiles were compared with the profiles of a standard amino acid solution and of cysteic acid, methionine sulfoxide, and methionine sulfone standards (Sigma). The recovery of tryptophan was determined after hydrolysis with 4 M methanesulfonic acid in the presence of 0.02% 3-(2-aminoethyl)indole (32). Cysteine and cystine residues were determined by quantification of their oxidation product following HCl hydrolysis in the presence of 0.2% sodium azide (28, 29).

Flux balance model. A bioreaction network with only branch point-associated metabolites was assembled for the calculation of intracellular fluxes. Network reactions in the central metabolism were constructed primarily from the established biochemistry in the literature (19, 42), and the biosynthetic pathway to riboflavin was constructed as described by Perkins and Pero (35) and Bacher (3). Formate formed during riboflavin biosynthesis, 3 mol of formate per mol of riboflavin, was considered to be converted to CO_2, because formate could not be detected in the fermentations. The gluconeogenic enzyme phosphoenolpyruvate carboxykinase was reported to be not active under the strict glucose-limited conditions used and was therefore not considered (12). Inclusion of the malic enzyme reaction does not affect any of the other net fluxes and was therefore not considered, in order to eliminate a potential cycle in the pyruvate shunt. Mass balances for CO_2 and NAD(P)H were also included in the model. Therefore, the reaction network consists of 23 metabolites and 21 reactions with unknown fluxes. A (pseudo)-steady-state approximation, in which the sum of the fluxes to and from any particular intermediary metabolite equals zero, was used for intracellular metabolite pools to generate the following linear mass balance equation for calculation of the flux distribution:

$$S \cdot v = b \tag{1}$$

In this representation, S is the stoichiometric bioreaction matrix (23×21) based on the metabolic map, v is the vector of 21 unknown metabolic fluxes to be determined, and b is the vector of 23 known fluxes from measurable products and substrates for each of the 23 metabolite balances. The solution to equation 1 was determined by a constrained least-squares approach with the objective of minimizing the sum of the squares of residuals from the metabolite mass balances. The only constraint in the least-squares problem was a demand for nonnegative fluxes in the irreversible reactions (v_1, v_7, v_{10}, v_{11}, and v_{12}). Sensitivity analysis on variations in biomass composition (relative protein, RNA, and cell wall content) and in production and consumption rates (within the confidence intervals) of the estimated fluxes was performed to analyze error propagation.

RESULTS

Determination of growth parameters. In this study, continuous cultivation in glucose-limited chemostats was used to determine the growth parameters of wild-type *B. subtilis* 1012 and the recombinant, riboflavin-producing strain PRF93. Steady-state data for both strains were obtained from several (11 and 4, respectively) independent cultivations, except the off-gas data for the wild-type, which were derived from 1 cultivation only. The experimental data on the continuous-growth physiology of both strains are in agreement with the chemostat model (37): steady-state specific glucose (q_{glc}) and oxygen (q_{O_2}) consumption rates, as well as the carbon dioxide evolution rate (q_{CO_2}), exhibit linear relationships with the specific growth rate (assuming $\mu = D$ at steady state), as shown in Fig. 1. The following equations were used for the calculation of the growth parameters in Table 1:

$$q = \frac{\mu}{Y^{max}} + m \tag{2}$$

where q is the specific rate of substrate consumption with respect to product formation, μ is the specific growth rate, Y^{max} is the maximum molar growth yield, and m is the maintenance coefficient (37, 39). When corrections were made to account for the glucose required for product formation, the following equation was used to determine $Y_{glc}^{max\ corr}$ and m^{corr} values (44):

$$q = \frac{\mu}{Y^{max\ corr}} + m^{corr} + aq_p$$

in which a is the amount of glucose required for the formation of 1 mol of product and q_p is the specific product formation rate. The linear regression lines in Fig. 1 were determined by a least-squares fit of the data.

Essentially identical maximum molar growth yields on glucose (Y_{glc}^{max}) of 82 and 83 g (dry weight) of cells per mol of glucose consumed were obtained for both strains as the inverse of the slope calculated by linear regression. This demonstrates an unchanged growth phenotype (Fig. 1A and D; Table 1). Correction of the PRF93 Y_{glc}^{max} for riboflavin formation results in a negligible increase. The maximum molar growth yield for oxygen ($Y_{O_2}^{max}$) was calculated and found to be virtually identical for both strains (Fig. 1B and E; Table 1). Experimental values for the maintenance coefficient (m), which can be ex-

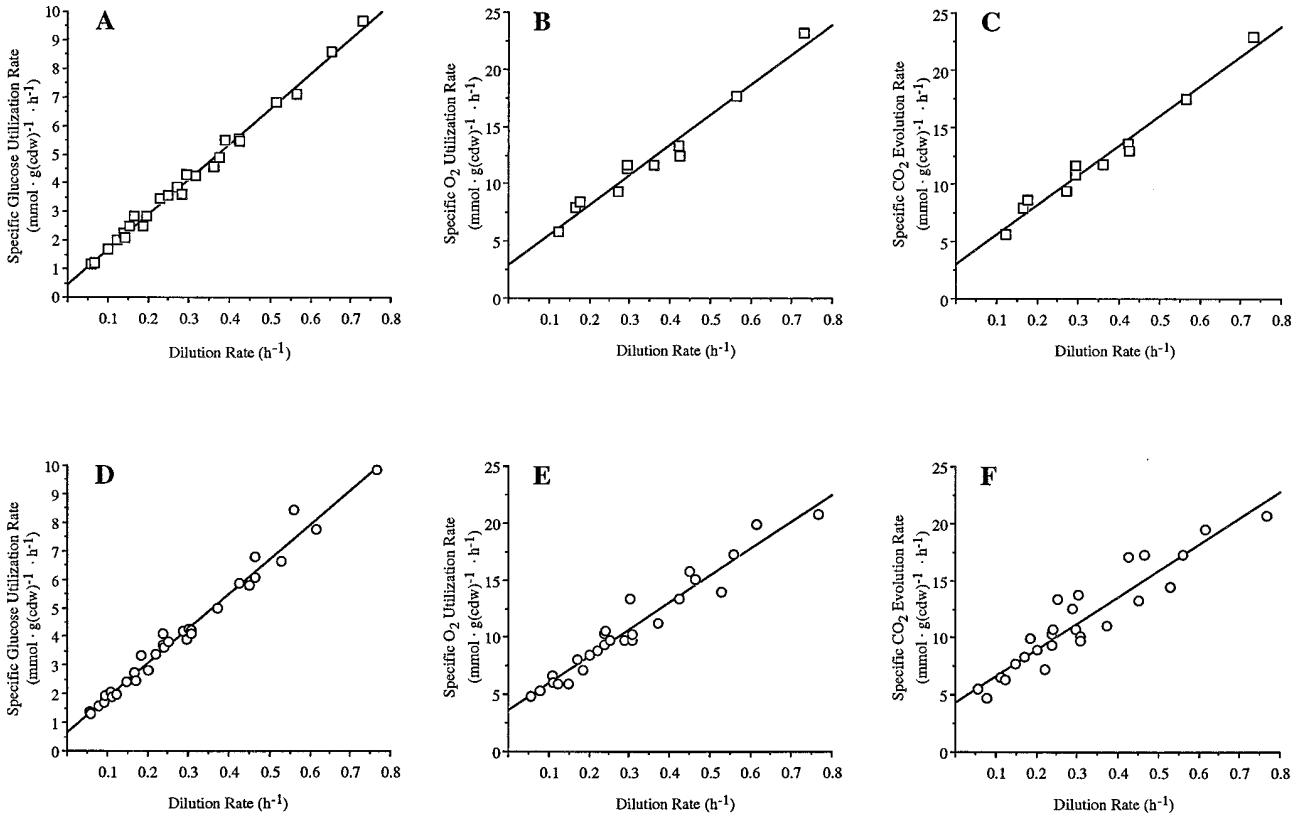

FIG. 1. Effect of dilution rate on the rates of glucose (A and D) and oxygen (B and E) consumption and carbon dioxide evolution (C and F) by *B. subtilis* 1012 (A to C) and PRF93 (D to F) during aerobic glucose-limited growth.

pressed as the substrate consumption rate (m_{glc} or m_{O_2}) or the CO_2 evolution rate (m_{CO_2}) required to fulfill the non-growth-associated demand, were determined by extrapolating the least-squares linear fit of the data to $\mu = 0$. The estimated m_{glc} values were relatively high, at 0.45 and 0.66 for the wild-type and overproducing strains, respectively (Table 1). A similarly high maintenance coefficient value was calculated by the method of Stouthamer and van Verseveld (46) for an overproducing strain in fed-batch cultivations (data not shown). Correcting for product formation has only a minor effect on this parameter. The increased maintenance metabolism for the recombinant strain, relative to the wild type, was also reflected in the m_{CO_2} value of this strain (50% increase). No metabolic overflow products were formed under the conditions investigated, and there was no residual glucose in the medium, on the basis of the minimum detection level of 1 mg/liter. The substrate carbon was quantitatively recovered in biomass, CO_2, and riboflavin. A carbon balance of 100% ± 3% was obtained at all reported growth rates.

Riboflavin formation in chemostat cultivation. The highest riboflavin concentrations in glucose-limited chemostat culture were found at dilution rate, D, between 0.2 and 0.45 h^{-1}, with a maximum at $D = 0.3$ h^{-1} (Fig. 2A). The specific riboflavin production rate increased up to $D = 0.45$ h^{-1}, when an essentially constant maximal level was reached, as shown in Fig. 2B. The product concentration in the medium was not only a function of D but also subject to a slow, constant decrease as a function of total volume changes (generations) in the chemostat. Therefore, only data points from cultures with fewer than 50 generations were considered, because riboflavin productivity did not decrease more than 20% at constant D to this point. However, independent of the chemostat generation, riboflavin production became highly unstable when D was below 0.15 h^{-1}. Stable production could be restored by subjecting these cultures to an intermediate batch cultivation with a 5% inoculation volume. Following this batch cultivation, these cultures

TABLE 1. Comparison of growth and maintenance parameters for *Bacillus* species

Parameter	Value[a] for:				
	B. subtilis			*B. licheniformis*[b]	
	1012 (wild type)	PRF93	168 (wild type)[c]	Non-protease producing	Protease producing
μ range (h^{-1})	0.05–0.75	0.05–0.75			0.05–0.35
$Y_{glc}^{max\,d}$	82 ± 2	83 ± 2	83	91 ± 2	84 ± 4
$Y_{glc}^{max\ corre}$		85 ± 2		97 ± 3	100 ± 6
$Y_{O_2}^{max}$	38 ± 3	42 ± 3		58 ± 13	53 ± 6
m_{glc}^{f}	0.45 ± 0.08	0.65 ± 0.10		0.14 ± 0.07	0.24 ± 0.11
m_{glc}^{corrf}		0.66 ± 0.11		0.16 ± 0.09	0.23 ± 0.12
$m_{CO_2}^{f}$	3.0 ± 0.6	4.4 ± 0.6		0.7 ± 0.5	1.6 ± 0.3
$m_{O_2}^{f}$	3.0 ± 0.6	3.6 ± 0.6		2.4 ± 1.3	1.1 ± 0.4
n^{g}	25 (11)	32 (26)			21

[a] The 95% confidence intervals based on the data shown in Fig. 1 are given.
[b] Data reported by Frankena et al. (17).
[c] Data reported by Santana et al. (41).
[d] Maximal molar growth yields expressed as grams (cellular dry weight) per mole of glucose or oxygen.
[e] Corrected for product formation.
[f] Maintenance coefficients expressed as micromoles per gram (cellular dry weight) per hour.
[g] The number of experiments used to calculate the parameters. Numbers in parentheses represent the experiments with off-gas analysis.

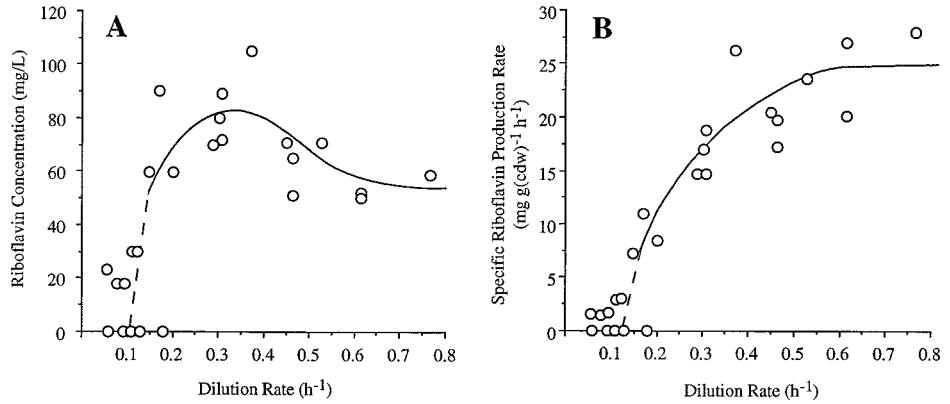

FIG. 2. Absolute riboflavin concentration (A) and specific riboflavin production rate (B) in steady states of continuous culture of *B. subtilis* PRF93. Dashed lines indicate unstable riboflavin production.

exhibited a stable but lower riboflavin production phenotype in chemostat cultivation (at D higher than 0.15 h^{-1}). Single colonies obtained from chemostat cultures that had lost riboflavin production at D lower than 0.15 h^{-1} were cultivated again in a chemostat. These chemostat cultures were phenotypically indistinguishable from PRF93 and produced normal riboflavin levels again, thus excluding a possible mutation mechanism. The presence of the PRF operon in all analyzed single colonies was also indicated by the unchanged tetracycline resistance of these cells.

Determination of monomeric cellular composition. To obtain the specific precursor requirements for *B. subtilis* biomass, we determined the total amino acid composition of logarithmically growing *B. subtilis* and *Escherichia coli* wild-type strains shown in Table 2. More than 50% of the bacterial biomass is made up of amino acids. The total amino acid composition determined for *E. coli* W3110 is very similar to the commonly used values for the amino acid composition of *E. coli* B reported by Neidhardt et al. (33). Significant variations are seen mainly for alanine and glutamate, because their peptidoglycan fraction was included in our analysis of total biomass. Several differences in the composition are evident when *E. coli* and *B. subtilis* are compared. In particular, the nonproteinogenic amino acid, diaminopimelate, yields useful information for precursor quantification of the gram-positive cell wall, which makes up a significant fraction of the dry weight and is clearly distinct from *E. coli*. Because diaminopimelate is used solely for cell wall synthesis, the value of 95 μmol/g of cellular dry weight can be used directly, with the known cell wall stoichiometry (2), to calculate the precursor requirements for cell wall formation. The higher relative portion of cell wall in *B. subtilis*, quantified through its diaminopimelate content, is also reflected in increased levels of the other monomeric cell wall components: alanine, glutamate, and glucosamine. However, the cell wall requirements for alanine and glutamate are relatively small in comparison with their protein fraction, and the determination of glucosamine was subject to significant hydrolysis losses. From the diaminopimelate data, we therefore conclude that the murein sacculus constitutes approximately 9% of *B. subtilis* biomass and that the relative contribution to total biomass is therefore three to five times higher than in *E. coli*. On the basis of the determined amino acid composition, as well as known *B. subtilis* physiology, we have quantified the detailed requirements for biomass building blocks in *B. subtilis* (Table 3). As lipopolysaccharides do not occur in the gram-positive bacilli, these requirements were not included. Peptidoglycan requirements were adjusted to the determined value of 95 μmol/g of cellular dry weight. The lipid composition of *B. subtilis* differs significantly from that of *E. coli*, since mainly branched fatty acids and phosphatidylglycerol are found (11, 24). On the basis of the determined molar amounts reported for *E. coli* (33), the following specific changes for lipid precursors of *B. subtilis* were therefore introduced: (i) an average acetyl coenzyme A requirement of 6.1 for fatty acids was calculated from Table 1 of de Mendoza et al. (11); (ii) valine was assumed to be the precursor for the branched C_{16} fatty acids; (iii) the precursors for odd-numbered

TABLE 2. Amino acid composition of *E. coli* and *B. subtilis*

Amino acid	Amt of amino acid (μmol/g [dry wt] of cells) in:		
	E. coli B/r[a] (in protein only)	*E. coli* W3110 (total)	*B. subtilis* 1012 (total)
Ala	488	527	594
Arg	281	273	198
Asx[b]	458	521	426
Cys	87	90[c]	60[c]
Glx[d]	500	580	639
Gly	582	578	495
His	90	93	86
Ile	276	272	288
Leu	428	420	368
Lys	326	304	342
Met	146	136	118
Phe	176	173	183
Pro	210	207	175
Ser	205	254[e]	239[e]
Thr	241	275[e]	239[e]
Trp	54	19[f]	0[f]
Tyr	131	143	125
Val	402	395	335
Total	5,081	5,260	4,910
Diaminopimelate	28[g]	19	95
Glucosamine	28[g]	32[f]	60[f]
Glycerol	129[g]	45	83

[a] Data from reference 33.
[b] Asparagine and aspartate.
[c] Determined as cystic acid.
[d] Glutamine and glutamate.
[e] Corrected for hydrolysis losses.
[f] Not corrected for hydrolysis losses.
[g] Determined indirectly.

TABLE 3. Specific precursor, cofactor, and CO_2 requirements for *B. subtilis* 1012

Precursor	Requirement (μmol/g [dry wt] of cells)[a]														
	G6P	F6P	R5P	E4P	T3P	PGA	PEP	Pyr	AcCoA	OaA	OGA	CO_2	ATP	NADH	NADPH
Protein[b]			86	308		794	616	2,440	368	1,413	917	−1,811	6,100	−1,743	10,302
RNA			630			368				262		−368	6,540	−1,366	1,163
DNA			100			50				50		−50	1,088	−200	300
Lipids					194	65		335	1,574	103		−568	1,419	−103	3,277
Peptidoglycan		190					95	285	190	95	95		855		760
Glycogen	154												154		
C_1 units						76						−76		−76	76
Polyamines											59		118		180
Total	154	190	816	308	194	1,353	711	3,060	2,132	1,923	1,071	−2,873	16,274	−3,488	16,058

[a] For definitions of abbreviations, see the legend to Fig. 3; negative values indicate formation.
[b] Murein fraction of alanine and glutamate subtracted and included in peptidoglycan.

branched fatty acids were assumed to be isoleucine and leucine in equal molar amounts (24); and (iv) a phospholipid composition of 25% phosphatidylethanolamine and 75% phosphatidylglycerol was used (11). As a result, the one-carbon (C_1) requirements were recalculated. When no specific information was available for *Bacillus* spp., the reported *E. coli* values (33) were used (e.g. DNA, RNA, glycogen, and polyamines). Furthermore, the experimentally determined elemental composition of *B. subtilis* 1012 and PRF93 harvested at various dilution rates revealed no growth rate or strain-specific variations and was as follows: C, 46 to 48%; H, 6.5 to 7%; and N, 12 to 13%. The calculated *B. subtilis* biomass composition is compared with that of *E. coli* in Table 4, and the actual values used for the flux analysis calculations are given in a separate column.

Estimation of metabolic fluxes. Information on metabolic fluxes is of the utmost importance for rational manipulation of microbial metabolism, and estimation of the intracellular carbon flux distribution from determination of extracellular products has become a standard technique (10, 18, 23, 38, 49–51). Such stoichiometric mass-balancing analyses depend upon precise knowledge of biochemical pathways, metabolic demands for growth, and optimization principles to predict the metabolic flux distribution within a defined network (Fig. 3).

NADPH was assumed to be produced only to fulfill biosynthetic requirements, and the NADH flux was set to equal the oxygen uptake. Experimental data on biomass and product formation rates, as well as on the CO_2 evolution rate and O_2 and glucose consumption rates, were used in combination with the monomeric cellular composition of *B. subtilis* given in Table 4. Values of the least-squares fits of the data from the chemostat experiments shown in Fig. 1 and 2 were used to estimate the production and consumption rates. The biosynthetic requirements for ribose-5-phosphate, 3-phosphoglycerate, and NAD(P)H, as well as the coupled CO_2 formation, were specified by the detailed requirements for phosphoribosyl diphosphate, IMP, GDP, and GTP.

The stoichiometric mass balance analysis employed provided an interpretation of the experimentally observed physiology by a quantitative description of the flux distribution within the defined bioreaction network and has several noteworthy characteristics. When specific growth rate and biomass yield (Y_{glc}) increased, an increased oxidative pentose phosphate pathway (PPP) flux (ν_1) was observed for the wild-type strain at the expense of the tricarboxylic acid (TCA) cycle flux (ν_{14}, ν_{15}, and ν_{16}) (Fig. 4). At dilution rates (D) of $\leq 0.1\ h^{-1}$, the oxidative branch of the PPP is not required any more. Similar patterns of PPP and TCA cycle utilization, as functions of dilution rate, were obtained for the riboflavin-producing strain. However, a noticeably higher PPP flux and lower TCA cycle flux were estimated for any given D. This behavior is caused mainly by the NADPH requirements for biosynthesis of the purine precursor. Flux values at $D \leq 0.05\ h^{-1}$ should be regarded as qualitative only, because the corresponding physiological data, obtained from extrapolating the relationships shown in Fig. 1, were not within the working range of a chemostat.

There is an uncertainty in the flux results obtained by this kind of metabolic stoichiometric analysis, because it depends on a priori assumptions regarding unknown features of the metabolic reaction network. In the particular case reported here, the most significant influence on the fluxes computed is exerted by the constraint that NADPH formation is strictly coupled to the biosynthetic NADPH requirements. This causes the PPP to operate only to satisfy the cellular requirements for NADPH and pentose precursors. Although supplying NADPH

TABLE 4. Building block and cofactor requirements for the formation of 1 g of *E. coli* and *B. subtilis* biomass

Precursor metabolite[a]	Amt required (μmol/g [dry wt] of cells)		
	E. coli B/r[b]	*B. subtilis* 1012	*B. subtilis* used in analysis[c]
G6P	205	154	154
F6P	71	190	190
R5P	898	816	
PRPP			398
IMP			190
GDP			25
GTP			203
E4P	361	308	308
T3P	129	194	194
PGA	1,496	1,353	726
PEP	719[d]	711	711
Pyr	2,833	3,060	3,060
AcCoA	2,928[d]	2,132	2,132
OGA	1,079	1,071	1,071
OaA	1,787	1,923	1,923
CO_2		−2,873	−3,082
ATP	18,485	16,274	
NADH	−3,547	−3,488	−2,215
NADPH	18,225	16,058	15,013

[a] For definitions of abbreviations, see the legend to Fig. 3.
[b] Data from reference 33.
[c] R5P and PGA requirements expressed as specific precursors corrected for cofactors.
[d] Corrected from reference 33.

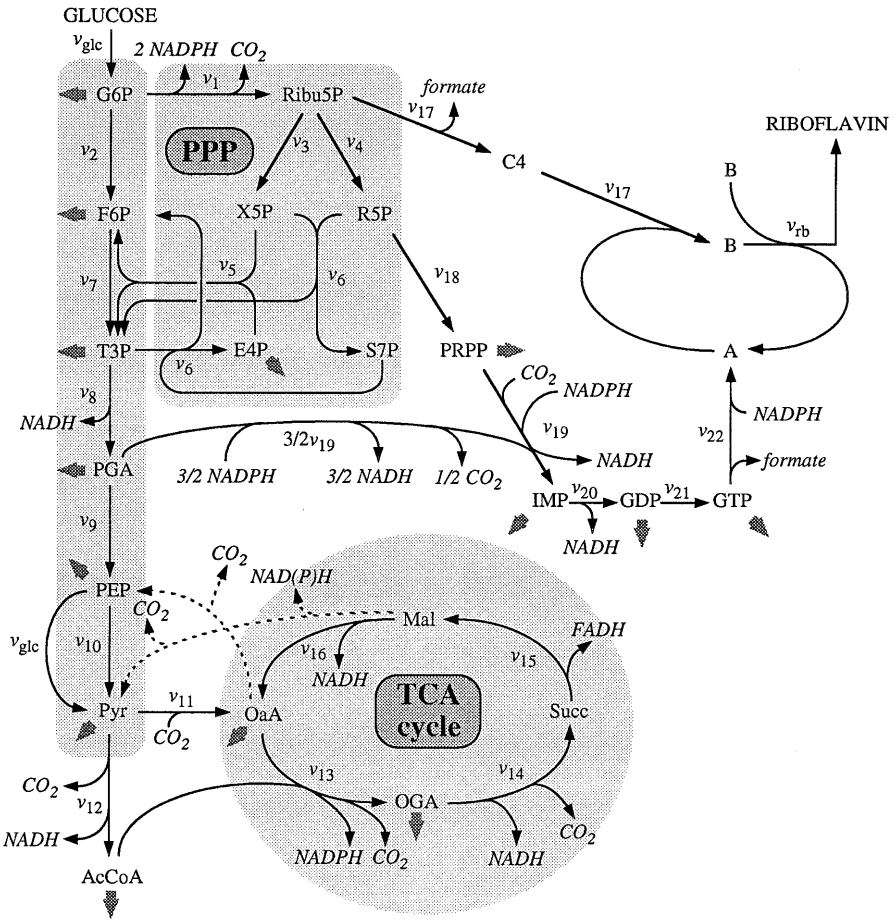

FIG. 3. The biochemical reaction network considered. The reactions illustrated by dashed arrows have not been included. Shaded arrows indicate the withdrawal of precursors for biosynthesis. The abbreviations A, B, and C4 represent 5-amino-6-(ribitylamino)-2,4-(1*H*,3*H*)-pyrimidinedione, 6,7-dimethyl-8-ribityllumazine, and 3,4-dihydroxy-2-butanone, respectively. Glycolytic, PPP, and TCA cycle reactions are shaded in grey. Abbreviations: G6P, glucose-6-phosphate; F6P, fructose-6-phosphate; T3P, triose-3-phosphate; PGA, 3-phosphoglyceric acid; PEP, phosphoenolpyruvate; Pyr, pyruvate; AcCoA, acetyl coenzyme A; Ribu5P, ribulose-5-phosphate; X5P, xylulose-5-phosphate; R5P, ribose-5-phosphate; E4P, erythrose-4-phosphate; S7P, seduheptulose-7-phosphate; PRPP, phosphoribosyl diphosphate; OaA, oxaloacetate; OGA, oxoglutarate.

and precursors is generally believed to be the primary biological function of the oxidative branch of the PPP, it has not been established that its operation is exclusively governed by this demand (15, 53). Phosphoglucoisomerase-negative mutants of *E. coli*, for example, metabolize glucose entirely through the PPP, as demonstrated by their ability to grow on glucose as the sole carbon source (16). Thus, these mutants must have mechanisms to reoxidize NADPH, other than the anabolic utilization of NADPH. Furthermore, PPP flux is generally reported to be in the range of 20 to 30% of the total glucose uptake in bacteria, which exceeds the biomass requirements for NADPH and pentose formation under many conditions (19, 33). Recently, by using labelling studies combined with metabolite balancing, it was shown for continuously growing, lysine-producing *Corynebacterium glutamicum* that the actual NADPH formation exceeded the biosynthetic requirements by 21.1% (30). Hence, the inclusion of this constraint may force the flux calculations to yield a biased solution in which all of the substrate carbon that is not accounted for in biomass and products will be converted to CO_2 in the TCA cycle.

In an attempt to obtain an unbiased estimate of this flux pattern, we assumed interchangeability of reducing equivalents, NADH and NADPH, which could be explained biologically by a transhydrogenase activity (19). In calculations performed with this assumption, the estimated oxidative PPP flux is significantly increased, reaching relative fluxes much higher than unity at the expense of the TCA cycle for all values of *D* (data not shown). A PPP flux higher than unity, however, would require a net recycling of fructose-6-phosphate into the PPP, and such behavior has not yet been described in the literature. If no further assumptions regarding the biological function of the PPP under these conditions are made, the estimated PPP flux is very sensitive to the respiratory quotient. At low *D*, for example, respiratory quotient values at or below unity result in increased flux through the oxidative branch of the PPP, whereas at values higher than unity, the same flux is estimated to be close to zero.

The actual flux distribution is most probably somewhere between the two above-described extremes. What may be the best current estimate was obtained by allowing a realistic 20% exchange of reducing equivalents from NADPH to NADH in the optimization calculations (Table 5), based on the experimental result of Marx et al. (30). The flux estimates obtained with this assumption for the PPP and TCA cycle (Fig. 5) are very similar to the solution shown in Fig. 4, indicating the robustness of the solution for a transfer of reducing equiva-

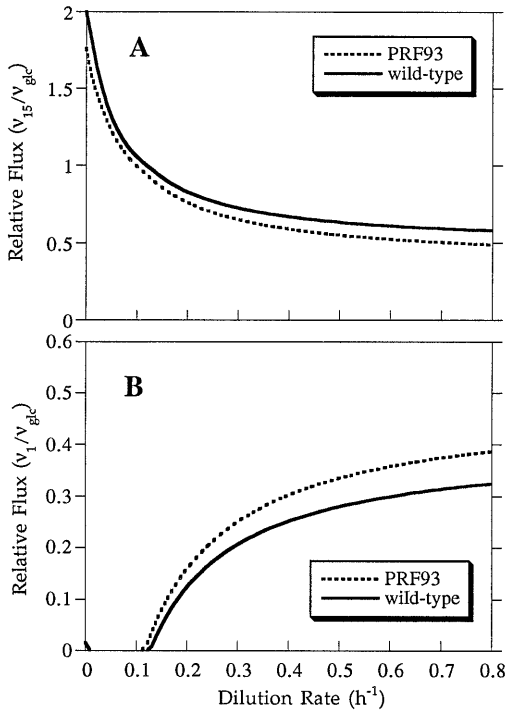

FIG. 4. Metabolic flux estimation for the TCA cycle (A) and the PPP (B) of wild-type and riboflavin-producing *B. subtilis*, assuming that NADPH formation is strictly coupled to biosynthetic requirements.

lents from NADPH to NADH in the physiological range. The estimated flux through the anaplerotic reaction (v_{11}) remained between 0.24 and 0.30 throughout the range of D investigated. The most pronounced difference was found for the PPP flux at higher D, which is estimated to reach values of around 50% instead of 30%. However, the dilution rate at which the PPP flux decreases to zero is not significantly affected. The relative differences between the strains are conserved in both solutions. The sensitivity analysis of the experimentally determined biomass composition and production and consumption rates indicated that within the confidence intervals, these input parameters had negligible effects on the flux estimates.

DISCUSSION

Growth parameters. Our physiological data are in good agreement with those obtained by other investigators for various *Bacillus* species, as shown in Table 1. In particular, the maximum molar growth yield reported for batch cultivation of *B. subtilis* (41) is almost identical to our findings. In contrast to the behavior of the facultative aerobic *B. licheniformis* (6, 17) and *E. coli* (51), our *B. subtilis* strain did not exhibit uncoupled growth at high growth rates in the glucose-limited chemostat, even when up to 100% higher glucose concentrations than those reported were used. This was demonstrated by the lack of metabolic overflow products detected in the culture supernatant. For *E. coli*, metabolic overflow in glucose-limited chemostat cultures is related to the low maximum O_2 utilization rate of 15 mmol of O_2 g (dry weight) of cells^{-1} h^{-1} (51), whereas in our experiments, the highest O_2 utilization rate was determined to be 22.5 mmol of O_2 g (dry weight) of cells^{-1} h^{-1}. Like *B. subtilis*, *B. licheniformis* is capable of O_2 utilization rates above 20 mmol of O_2 g (dry weight) of cells^{-1} h^{-1} but has a comparatively low μ_{max} of 0.6 h^{-1} (6). Metabolic uncoupling in *B. licheniformis* at $D \geq 0.3$ h^{-1} (50 to 100% of μ_{max}) is presumably necessary to produce the higher rates of ATP turnover required to sustain higher biosynthesis (growth) rates. Additionally, the metabolic burden associated with substantial extracellular protein formation, which consumes 10 to 20% of the glucose input (17), potentially could further increase metabolic overflow.

The maintenance coefficient for glucose of 0.45 determined for wild-type *B. subtilis* is high compared with those for *B. licheniformis* (17) and *E. coli* (48, 51) of 0.14 to 0.24 and 0.17 to 0.30, respectively. This finding indicates that *B. subtilis* devotes a relatively high portion of its energy supply to maintenance metabolism, possibly for cell wall turnover (45). This observation is further strengthened by the lower maximal biomass yield on glucose and oxygen when compared with *B. licheniformis* (Table 1). This has significant implications for biotechnological applications. Industrial-scale fermentations under conditions of very slow growth, such as the commonly used fed-batch cultivation, are very sensitive to maintenance requirements, since the relative importance of maintenance requirements increases at lower growth rates (46). Thus, the m_{glc} determined for wild-type *B. subtilis* is a clear illustration of the influence of the intrinsic physiological properties of a microorganism on productivity in bioreactors.

A significant (47%) increase in the maintenance coefficient was found for the riboflavin-producing strain PRF93 despite an essentially wild-type molar growth yield. The glucose required for maintenance in both strains is almost completely burned to CO_2, because the molar m_{CO_2} values observed are approximately 6 times the m_{glc} values expected for complete conversion of glucose to CO_2. It should be recognized that in the relationship between growth yield and growth rate (equation 2), all of the energy not used for growth is included in the maintenance term (m). Therefore, factors that are by defini-

TABLE 5. Estimated fluxes, normalized to glucose uptake, for various dilution rates in continuous culture of wild-type and riboflavin-producing *B. subtilis* strains

Flux[a]	Value of flux for D value of[b]:			
	0.1 h^{-1}	0.3 h^{-1}	0.5 h^{-1}	0.7 h^{-1}
v_1	0.03, 0.04	0.34, 0.38	0.42, 0.47	0.45, 0.51
v_2	0.97, 0.95	0.65, 0.61	0.58, 0.52	0.54, 0.48
v_3	−0.02, −0.04	0.17, 0.17	0.22, 0.23	0.24, 0.26
v_4	0.07, 0.08	0.19, 0.20	0.22, 0.24	0.23, 0.26
v_5	−0.02, −0.03	0.07, 0.07	0.10, 0.10	0.11, 0.12
v_6	0.00, −0.01	0.10, 0.10	0.12, 0.13	0.13, 0.14
v_7	0.95, 0.89	0.81, 0.77	0.78, 0.74	0.76, 0.72
v_8	1.85, 1.75	1.68, 1.60	1.64, 1.56	1.62, 1.54
v_9	1.73, 1.60	1.52, 1.42	1.46, 1.37	1.44, 1.35
v_{10}	0.68, 0.55	0.46, 0.36	0.40, 0.31	0.38, 0.28
v_{11}	0.24, 0.21	0.29, 0.28	0.30, 0.30	0.31, 0.30
v_{12}	1.25, 1.17	0.94, 0.86	0.86, 0.77	0.82, 0.73
v_{13}	1.13, 1.06	0.79, 0.71	0.70, 0.61	0.66, 0.57
v_{14}	1.04, 0.98	0.68, 0.61	0.59, 0.51	0.55, 0.46
v_{15}	1.04, 0.98	0.68, 0.61	0.59, 0.51	0.55, 0.46
v_{16}	1.04, 0.98	0.68, 0.61	0.59, 0.51	0.55, 0.46
v_{17}	0.00, 0.00	0.00, 0.02	0.00, 0.02	0.00, 0.02
v_{18}	0.07, 0.09	0.10, 0.11	0.10, 0.11	0.10, 0.12
v_{19}	0.05, 0.07	0.07, 0.08	0.07, 0.08	0.08, 0.09
v_{20}	0.02, 0.04	0.03, 0.05	0.04, 0.05	0.04, 0.05
v_{21}	0.02, 0.04	0.03, 0.05	0.04, 0.05	0.04, 0.05
v_{22}	0.00, 0.00	0.00, 0.01	0.00, 0.01	0.00, 0.01

[a] Fluxes correspond to the labels used in Fig. 3.
[b] Values for the wild-type strain are followed by values for the riboflavin-producing strain.

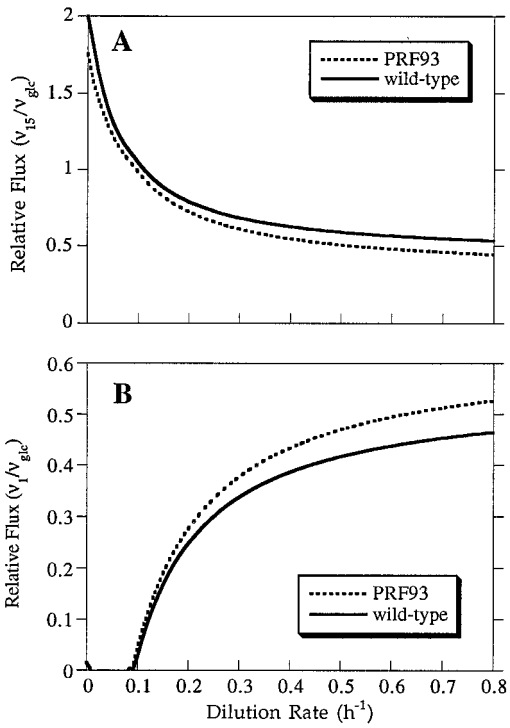

FIG. 5. Metabolic flux estimation for the TCA cycle (A) and the PPP (B) of wild-type and riboflavin-producing *B. subtilis*, assuming up to 20% transfer of NADPH reducing equivalents to NADH.

tion not maintenance processes, such as potential spilling mechanisms, form part of the parameter *m*, as deduced from a linear regression of substrate uptake rate against growth rate (37, 39, 47). The formation of riboflavin per se cannot account for the increased maintenance coefficient in the overproducing strain, since 50 to 100 mg of riboflavin per liter, corresponding to 2.3 to 4.7% of the supplied glucose (on a molar basis), was produced under the strict carbon-limited conditions used. This is illustrated by the minor change in the product-corrected m_{glc}^{corr} for PRF93 in Table 1. The macromolecular burden of protein synthesis (4) can be excluded from having a substantial impact on the maintenance parameter, since the riboflavin biosynthetic enzyme levels in our strain did not significantly exceed 1% of the total cellular protein (data not shown). In this connection, it is interesting that elevated temperatures may perturb a normal metabolic balance, driving higher maintenance at essentially unchanged growth yields (13, 27, 34, 52), as was observed in the present study following the production of a relatively small amount of riboflavin. The most likely explanation for this effect is a metabolic perturbation, caused by riboflavin formation, potentially in the purine nucleotide availability. Alternatively, the presence of the *ribC* mutation in the riboflavin-producing strain might contribute to increased maintenance metabolism through effects other than regulation of the levels of the riboflavin biosynthetic enzymes. Pleiotropic effects of the *ribC* mutation cannot be excluded, since this protein functions not only as a repressor of *rib* gene expression but also as a flavin kinase. In the latter function, this enzyme converts riboflavin to the coenzymes flavin mononucleotide and flavin adenine dinucleotide (8). Furthermore, it is also possible that the defective *bpr* gene in PRF93 contributes to the increased maintenance requirements. The nature of this significant increase in maintenance requirements will be the subject of further investigations.

Riboflavin formation. The specific riboflavin production rate is apparently positively correlated with the growth rate under strict glucose-limited conditions and is thus coupled to growth. For *D* between 0.1 and 0.15 h^{-1}, strain PRF93 is not able to stably maintain riboflavin production. The nature of this instability is not clear. However, under similar conditions, bacterial cells are known to enter a growth rate domain that is dominated by maintenance energy demands (7). The resulting energy limitation reduces the phosphorylation potential within the cells. Thus, it is tempting to speculate that the limited availability of the GTP precursor, and not a decreased flux through the purine biosynthesis pathway, would limit riboflavin formation. In bacilli, the normal response to decreasing guanine nucleotide levels is the initiation of sporulation (26), which is prevented by a *spo0A* mutation in our strain. These results also suggest that for desirable production in a glucose-limited fed-batch process, the feeding profile should be designed in such a way as to maintain a minimal specific growth rate above 0.15 h^{-1}.

Flux analysis. The first and to our knowledge the only other report on metabolic flux patterns in *B. subtilis* was based on a similar stoichiometric approach by Goel et al. (18). Under continuous-culture conditions that were comparable to our experiments, a TCA cycle flux in the range of 1.3 to 1.5 (normalized to glucose uptake) and a PPP flux close to zero were estimated for three different steady states (D = 0.15, 0.3, and 0.5 h^{-1}). This completely different flux pattern (compare with Fig. 4 and 5) can be explained by several differences between the mass balance equations used (18) compared with our system: (i) the energetic requirements for glucose uptake were considered in terms of ATP equivalents instead of the phosphoenolpyruvate-dependent phosphotransferase system; (ii) isocitrate dehydrogenase was defined as the major source of NADPH, causing the oxidative PPP to be utilized only when this reaction could not fulfill the NADPH demand; (iii) no O_2 data were used, so that NAD(P)H balances depended only on glucose uptake and biomass formation; and (iv) a different biomass composition was used. From our data, we conclude that at higher *D* there is a substantial flux (30 to 50%) through the PPP in *B. subtilis*. The apparent reduction of PPP utilization at low *D* in both strains is strongly influenced by the assumed coupling of NADPH production with biosynthetic requirements in combination with lower biomass yields and is therefore likely to be underestimated. However, similar results showing relatively lower oxidative PPP flux under conditions of slow growth were obtained from [^{14}C]glucose and [^{18}O]glucose experiments with *E. coli* (25, 31).

Estimation of metabolic fluxes based on stoichiometric models is without doubt a valuable and easy-to-use tool. Nevertheless, the uncertainties arising from assumptions about imprecisely understood biological functions clearly illustrate the problems inherent in a purely stoichiometric flux analysis. Such an analysis is predicated on the assumption (among others) that all of the reactions involving the metabolites considered are known in vivo under the conditions used. As many reactions in the central metabolism, such as coupling of NADPH formation to biosynthetic requirements, operation of futile cycles, and slippage in membrane energy transduction, are not yet fully understood, there will be considerable uncertainty in some of the flux estimates derived from a strictly stoichiometric mass balance analysis. If, for example, the PPP in *B. subtilis* is a minor source of NADPH, as was shown for *E. coli* (9), our PPP flux estimates would be too high. The flux estimates presented here should therefore be viewed as approximations that are consistent with the data. While the absolute flux distribution may still be uncertain to some degree, the relative differ-

ences between the strains are probably realistic estimates. The estimated flux differences between the strains are rather small but nevertheless are significant, since only a small difference exists between the two strains in terms of Y_{glc} and product formation under the conditions used. Despite the tenor of the preceding discussion, we do not advocate avoiding mass balance-based analysis but, rather, wish to enhance the awareness of its limitations and to avoid assumptions about metabolic functions whenever possible.

ACKNOWLEDGMENTS

This work was supported by the Swiss Priority Program in Biotechnology (SPP Biotechnology).

The help of EAWAG (Zürich, Switzerland) in obtaining the CHN composition of our cells is gratefully acknowledged. We thank Dan R. Lasko for critical reading of the manuscript.

REFERENCES

1. **Arbige, M. V., B. A. Bulthuis, J. Schultz, and D. Crabb.** 1993. Fermentation of *Bacillus*, p. 871–895. *In* A. L. Sonenshein, J. A. Hoch, and R. Losick (ed.), *Bacillus subtilis* and other gram-positive bacteria: biochemistry, physiology, and molecular genetics. American Society for Microbiology, Washington, D.C.
2. **Archibald, A. R., I. C. Hancock, and C. R. Harwood.** 1993. Cell wall structure, synthesis, and turnover, p. 381–410. *In* A. L. Sonenshein, J. A. Hoch, and R. Losick (ed.), *Bacillus subtilis* and other gram-positive bacteria: biochemistry, physiology, and molecular genetics. American Society for Microbiology, Washington, D.C.
3. **Bacher, A.** 1991. Biosynthesis of flavins, p. 215–259. *In* F. Müller (ed.), Chemistry and biochemistry of flavoenzymes, vol. 1. CRC Press, Inc., Boca Raton, Fla.
4. **Bailey, J. E.** 1993. Host-vector interactions in *Escherichia coli*. Adv. Biochem. Eng. Biotechnol. **48:**29–52.
5. **Bergmeyer, H. U.** 1985. Methods of enzymatic analysis, vol. IV. VCH Publishers, Deerfield Beach, Fla.
6. **Bulthuis, B. A., G. M. Koningstein, A. H. Stouthamer, and H. W. van Verseveld.** 1989. A comparison between aerobic growth of *Bacillus licheniformis* in continuous culture and partial-recycling fermentor, with contributions to the discussion on maintenance energy demand. Arch. Microbiol. **152:**499–507.
7. **Chesbro, W., M. Arbige, and R. Eifert.** 1990. When nutrient limitation places bacteria in the domains of slow growth: metabolic, morphologic, and cell cycle behavior. FEMS Microbiol. Ecol. **74:**103–119.
8. **Coquard, D., M. Huccas, M. Ott, J. M. van Dijl, A. P. G. M. van Loon, and H.-P. Hohmann.** The riboflavin regulatory gene *ribC* has significant homology to flavin kinase and FAD synthase. Submitted for publication.
9. **Csonka, L. N., and D. G. Fraenkel.** 1977. Pathways of NADPH formation in *Escherichia coli*. J. Biol. Chem. **252:**3382–3391.
10. **de Hollander, J. A.** 1991. Application of a metabolic balancing technique to the analysis of microbial fermentation data. Antonie Leeuwenhoek **60:**275–292.
11. **de Mendoza, D., R. Grau, and J. E. Cronan, Jr.** 1993. Biosynthesis and function of membrane lipids, p. 411–421. *In* A. L. Sonenshein, J. A. Hoch, and R. Losick (ed.), *Bacillus subtilis* and other gram-positive bacteria: biochemistry, physiology, and molecular genetics. American Society for Microbiology, Washington, D.C.
12. **Diesterhaft, M. D., and E. Freese.** 1973. Role of pyruvate carboxylase, phosphoenolpyruvate carboxykinase, and malic enzyme during growth and sporulation of *Bacillus subtilis*. J. Biol. Chem. **248:**6062–6070.
13. **Farmer, I. S., and C. W. Jones.** 1976. The effect of temperature on the molar growth yield and maintenance requirement of *Escherichia coli* W during aerobic growth in continuous culture. FEBS Lett. **67:**359–363.
14. **Florent, J.** 1986. Vitamins, p. 115–157. *In* G. Reed and H.-J. Rehm (ed.), Biotechnology, vol. 4. VCH Verlagsgesellschaft, Weinheim, Germany.
15. **Fraenkel, D. G.** 1987. Glycolysis, pentose phosphate pathway, and Entner-Doudoroff pathway, p. 142–150. *In* F. C. Neidhardt, J. L. Ingraham, K. B. Low, B. Magasanik, M. Schaechter, and H. E. Umbarger (ed.), *Escherichia coli* and *Salmonella typhimurium*: cellular and molecular biology. American Society for Microbiology, Washington, D.C.
16. **Fraenkel, D. G., and R. T. Vinopal.** 1973. Carbohydrate metabolism in bacteria. Annu. Rev. Microbiol. **27:**69–100.
17. **Frankena, J., H. W. van Verseveld, and A. H. Stouthamer.** 1985. A continuous culture study of the bioenergetic aspects of growth and production of exocellular protease in *Bacillus licheniformis*. Appl. Microbiol. Biotechnol. **22:**169–176.
18. **Goel, A., J. Ferrance, J. Jeong, and M. M. Ataai.** 1993. Analysis of metabolic fluxes in batch and continuous cultures of *Bacillus subtilis*. Biotechnol. Bioeng. **42:**686–696.
19. **Gottschalk, G.** 1986. Bacterial metabolism, 2nd ed. Springer-Verlag, New York.
20. **Harwood, C. R.** 1992. *Bacillus subtilis* and its relatives: molecular biological workhorses. Trends Biotechnol. **10:**247–256.
21. **Harwood, C. R., and S. M. Cutting.** 1990. Molecular biological methods for *Bacillus*. John Wiley & Sons, Chichester, England.
22. **Heijnen, J. J., J. A. Roels, and A. H. Stouthamer.** 1979. Application of balancing methods in modeling the penicillin fermentation. Biotechnol. Bioeng. **21:**2175–2201.
23. **Holms, W. H.** 1986. The central metabolic pathways of *Escherichia coli*: relationship between flux and control at a branch point, efficiency of conversion to biomass, and excretion of acetate. Curr. Top. Cell. Regul. **28:**69–105.
24. **Kaneda, T.** 1991. Iso- and anteiso-fatty acids in bacteria: biosynthesis, function, and taxonomic significance. Microbiol. Rev. **55:**288–302.
25. **Katz, J., and R. Rognstad.** 1967. The labeling of pentose phosphate from glucose-^{14}C and estimation of the rates of transaldolase, transketolase, the contribution of the pentose cycle, and ribose phosphate synthesis. Biochemistry **6:**2227–2247.
26. **Lopez, J. M., C. L. Marks, and E. Freese.** 1979. The decrease of guanine nucleotides initiates sporulation of *Bacillus subtilis*. Biochim. Biophys. Acta **587:**238–252.
27. **Mainzer, S. E., and W. P. Hempfling.** 1976. Effects of growth temperature on yield and maintenance during glucose-limited continuous culture of *Escherichia coli*. J. Bacteriol. **126:**251–256.
28. **Manneberg, M., H.-W. Lahm, and M. Fountoulakis.** 1995. Oxidation of cysteine and methionine residues during acid hydrolysis of proteins in the presence of sodium azide. Anal. Biochem. **224:**122–127.
29. **Manneberg, M., H.-W. Lahm, and M. Fountoulakis.** 1995. Quantification of cysteine residues following oxidation to cysteic acid in the presence of sodium azide. Anal. Biochem. **231:**349–353.
30. **Marx, A., A. A. de Graaf, W. Wiechert, L. Eggeling, and H. Sahm.** 1996. Determination of the fluxes in the central metabolism of *Corynebacterium glutamicum* by nuclear magnetic resonance spectroscopy combined with metabolite balancing. Biotechnol. Bioeng. **49:**111–129.
31. **Model, P., and D. Rittenberg.** 1967. Measurement of the activity of the hexose monophosphate pathway of glucose metabolism with the use of [^{18}O] glucose. Variations in its activity in *Escherichia coli* with growth conditions. Biochemistry **6:**69–79.
32. **Moore, S.** 1972. Chemistry and biology of peptides, p. 629–653. *In* J. Melenhofer (ed.), Proteins. Ann Arbor Publishers, Ann Arbor, Mich.
33. **Neidhardt, F. C., J. L. Ingraham, and M. Schaechter.** 1990. Physiology of the bacterial cell: a molecular approach. Sinauer Associates, Inc., Sunderland, Mass.
34. **Pennock, J., and D. W. Tempest.** 1988. Metabolic and energetic aspects of the growth of *Bacillus stearothermophilus* in glucose-limited and glucose-sufficient chemostat culture. Arch. Microbiol. **150:**452–459.
35. **Perkins, J. B., and J. G. Pero.** 1993. Biosynthesis of riboflavin, biotin, folic acid, and cobalamin, p. 319–334. *In* A. L. Sonenshein, J. A. Hoch, and R. Losick (ed.), *Bacillus subtilis* and other gram-positive bacteria: biochemistry, physiology, and molecular genetics. American Society for Microbiology, Washington, D.C.
36. **Perkins, J. B., J. G. Pero, and A. Sloma.** 1991. Riboflavin overproducing strains of bacteria. European patent application 0-405-370-A1.
37. **Pirt, S. J.** 1965. The maintenance energy of bacteria in growing cultures. Proc. R. Soc. London Ser. B. **163:**224–231.
38. **Reardon, K., T.-H. Scheper, and J. E. Bailey.** 1987. Metabolic pathway rates and culture fluorescence in batch fermentations of *Clostridium acetobutylicum*. Biotechnol. Prog. **3:**153–167.
39. **Russell, J. B., and G. M. Cook.** 1995. Energetics of bacterial growth: balance of anabolic and catabolic reactions. Microbiol. Rev. **59:**48–62.
40. **Saito, H., T. Shibaat, and T. Ando.** 1979. Mapping of genes determining nonpermissiveness and host specific restriction to bacteriophages in *Bacillus subtilis* Marburg. Mol. Gen. Genet. **170:**117–122.
41. **Santana, M., M. S. Ionescu, A. Vertes, R. Longin, F. Kunst, A. Danchin, and P. Glaser.** 1994. *Bacillus subtilis* F_0F_1 ATPase: DNA sequence of the *atp* operon and characterization of *atp* mutants. J. Bacteriol. **176:**6802–6811.
42. **Sonenshein, A. L., J. A. Hoch, and R. Losick (ed.).** 1993. *Bacillus subtilis* and other gram-positive bacteria: biochemistry, physiology, and molecular genetics. American Society for Microbiology, Washington, D.C.
43. **Spackman, D. H., W. H. Stein, and S. Moore.** 1958. Automatic recording apparatus for use in the chromatography of amino acids. Anal. Chem. **30:**1190–1206.
44. **Stouthamer, A. H.** 1979. The search for correlation between theoretical and experimental growth yields, p. 1–48. *In* J. R. Quayle (ed.), Microbial biochemistry, vol. 21. University Park Press, Baltimore.
45. **Stouthamer, A. H., and C. Bettenhausen.** 1973. Utilization of energy for growth and maintenance in continuous and batch cultures of microorganisms. Biochim. Biophys. Acta **301:**53–70.
46. **Stouthamer, A. H., and H. W. van Verseveld.** 1987. Microbial energetics should be considered in manipulating metabolism for biotechnological purposes. Trends Biotechnol. **5:**149–155.

47. **Tempest, D. W., and O. M. Neijssel.** 1984. The status of Y_{ATP} and maintenance energy as biological interpretable phenomena. Annu. Rev. Microbiol. **38:**459–486.
48. **Tempest, D. W., and O. M. Neijssel.** 1987. Growth yield and energy distribution, p. 797–806. *In* F. C. Neidhardt, J. L. Ingraham, K. B. Low, B. Magasanik, M. Schaechter, and H. E. Umbarger (ed.), *Escherichia coli* and *Salmonella typhimurium*: cellular and molecular biology. American Society for Microbiology, Washington, D.C.
49. **Vallino, J., and G. Stephanopoulos.** 1990. Flux determination in cellular bioreaction network: application to lysine fermentation, p. 205–219. *In* S. K. Sikdar, M. Bier, and P. Todd (ed.), Frontiers in bioprocessing. CRC Press, Inc., Boca Raton, Fla.
50. **Varma, A., and B. O. Palsson.** 1994. Metabolic flux balancing: basic concepts, scientific, and practical use. Bio/Technology **12:**994–998.
51. **Varma, A., and B. O. Palsson.** 1994. Stoichiometric flux balance models quantitatively predict growth and metabolic by-product secretion in wild-type *Escherichia coli* W3110. Appl. Environ. Microbiol. **60:**3724–3731.
52. **Wallace, R. J., and W. H. Holms.** 1986. Maintenance coefficients and rates of turnover of cell material in *Escherichia coli* ML308 at different growth temperatures. FEMS Microbiol. Lett. **37:**317–320.
53. **Wood, T. D.** 1985. The pentose phosphate pathway. Academic Press, Inc., Orlando, Fla.